# Isoliquiritigenin modulates the activity of LTS and non-LTS cells in the ventrolateral preoptic area via GABA$_A$ receptors

Sumei Fan [a,b], Qiaoling Jin [b], Pingping Zhang [b], Dejiao Xu [b], Juan Cheng [b,**], Liecheng Wang [a,b,c,*]

[a] Department of Anatomy and Histoembryology, School of Basic Medical Sciences, Anhui Medical University, Hefei, China
[b] Department of Physiology, School of Basic Medical Sciences, Anhui Medical University, Hefei, China
[c] School of Stomatology, Anhui Medical University, Hefei, Anhui, China

## ARTICLE INFO

## ABSTRACT

*Objective:* Isoliquiritigenin (ILTG) is a chalcone compound that exhibits hypnotic effects via gamma-aminobutyric acid type A (GABA$_A$) receptors. The ventrolateral preoptic area (VLPO) is a sleep-promoting center that contains a large number of GABA-releasing cells. There are two cell types in the VLPO: one generates a low-threshold spike (LTS), whereas the other lacks an LTS (non-LTS).
*Method:* Whole-cell patch-clamp technology was used to detect the firing and currents of LTS and non-LTS cells in the VLPO.
*Results:* Bath administration of ILTG (10 μM) increased the firing rate of VLPO LTS cells, reversed by flumazenil (5 μM), a GABA$_A$ benzodiazepine site antagonist. However, the firing rate of VLPO non-LTS cells was inhibited by ILTG (10 μM), also reversed by flumazenil (5 μM). No differences were detected regarding resting membrane potential (RMP) amplitude, spike threshold, after-hyperpolarization (AHP) amplitude, or action potential duration (APD$_{50}$) after ILTG (10 μM) perfusion in VLPO LTS cells. RMP amplitude was more hyperpolarized and spike threshold was higher after ILTG (10 μM) application in VLPO non-LTS cells. In addition, ILTG significantly reduced the frequency of miniature inhibitory postsynaptic currents (mIPSCs) in VLPO LTS cells. ILTG significantly increased the amplitude of mIPSCs in VLPO non-LTS cells.
*Conclusions:* This study revealed that ILTG suppresses presynaptic GABA release on VLPO LTS cells, thereby increasing their excitability. ILTG enhances postsynaptic GABA$_A$ receptor function on VLPO non-LTS cells, thereby decreasing their excitability. These results suggest that ILTG may produce hypnotic effects by modulating the GABAergic synaptic transmission properties of these two cell types.

* Corresponding author. Department of Anatomy and Histoembryology and department of Physiology, Anhui Medical University, NO. 81, Meishan Road, Shushan District, Hefei, Anhui, 230032, China.
** Corresponding author. Department of Physiology, Anhui Medical University, NO. 81, Meishan Road, Shushan District, Hefei, Anhui, 230032, China.
*E-mail addresses:* JuanCheng@ahmu.edu.cn (J. Cheng), wangliecheng2022@163.com (L. Wang).

## 1. Introduction

Isoliquiritigenin (ILTG) is a chalcone compound widely found in plants such as glycyrrhiza and peanut stems [1,2]. ILTG has many potent pharmacological effects, including being anticancer, anti-inflammatory, and antiallergic [3–5]. Additionally, ILTG exhibits many neurological functions, including neuroprotective, and antioxidant functions, possibly by acting on vasopressin V1$_A$, dopamine D1, and D3 receptors [6–8]. Also, anxieties caused by persistent nicotine withdrawal symptoms are suppressed by ILTG [9,10]. It has been reported that high concentrations of anxiolytic-containing compounds may have hypnotic effects [11]. According to Cho et al., ILTG exerts hypnotic effects by gamma-aminobutyric acid type A (GABA$_A$) receptors [12]. Studies have indicated that ILTG has a potential role in modulating GABAergic synaptic transmission [12,13]. However, the influence of ILTG on the cells of the ventrolateral preoptic area (VLPO) remains unclear.

The VLPO plays an irreplaceable role in sleep-wake regulation, mainly by promoting non-rapid eye movement (NREM) sleep [14–17]. In addition, electrophysiological recordings have indicated that two cell types are present in the VLPO [18,19]. Low-threshold spike (LTS) is a characteristic of LTS cells, which account for approximately two-thirds of the VLPO and exhibit a multipolar triangular morphology [18,19]. Studies have shown that LTS cells exhibit sleep-promoting effects [18–20]. Moreover, most of the LTS cells co-release GABA and galanin [21]. However, the cells that lack an LTS, named non-LTS cells, with bipolar morphology play a role in promoting wakefulness [18,19,22]. Previous studies have indicated that the VLPO contains a large number of GABA-releasing cells, of which LTS and non-LTS cells are GABAergic [21,23]. GABAergic synaptic transmission in the VLPO regulates the sleep-wake state [21,23]. Studies have shown that acutely activated wake-promoting GABAergic neurons in the lateral hypothalamus and the galaninergic neurons in the VLPO are inhibited, resulting in arousal [23–25]. In addition, studies have shown that orexin, histamine, and other wake-up signals may inhibit galaninergic neurons in the VLPO via internal GABAergic circuits [19,22, 26–28]. Studies have indicated that ILTG has a potential role in modulating GABAergic synaptic transmission [12,13].

Thus, we hypothesized that ILTG might modulate the activity of LTS and non-LTS cells in the VLPO via GABA$_A$ receptors.

## 2. Materials and methods

### 2.1. Animals

Male SPF C57BL/6J mice aged between 4 and 5 weeks were used. The mice were housed in a room kept at $22 \pm 2$ °C with an automated 12-h dark/light (D/L) cycle. Water and food were available. We followed the regulations on the management of experimental animals of the People's Republic of China and the methods for quality management of experimental animals. Ethical approval for this study (No. LLSC20190763) was provided by the Institutional Animal Care Unit Committee of Anhui Medical University on October 10, 2019.

### 2.2. Chemicals

Isoliquiritigenin was purchased from Sigma (13766). Flumazenil was purchased from Sigma (1273808). Noradrenaline was purchased from Acmec (69815-49-2). Tetrodotoxin (TTX) was purchased from Bailingwei J&K (608506). CNQX was purchased from abcam (ab120017). D-AP5 was purchased from abcam (ab144482). All other chemicals were purchased from Sigma.

### 2.3. Preparation of brain slices

Male mice (4–5 weeks) were deeply anesthetized with 0.04 % isoflurane and later sacrificed. The brains were quickly extracted and moved in ice-cold N-methyl-D-glucamine (NMDG) cutting solution, which contained (in mM) 92 NMDG, 30 NaHCO$_3$, 1.2 KCl, 25 D-glucose, 1.2 KH$_2$PO$_4$, 5 L-ascorbic acid, 20 HEPES, 2 thiourea, 3 Na-pyruvate, 0.5 CaCl$_2$, and 1 MgSO$_4$ (pH: $7.2 \pm 0.1$; osmolarity: 310 $\pm$ 5 mOsm kg$^{-1}$). The solution was filled with 95 % O$_2$/5 % CO$_2$ for approximately 10 min, and then placed in a refrigerator to freeze into ice-cold compound prior to use. We used a vibrating microtome (VT1200s, Leica) to cut the brains in coronal planes of approximately 300 μm thickness at 0.18 mm s$^{-1}$ and then bred in artificial cerebrospinal fluid (aCSF) bubbled with 95 % O$_2$/5 % CO$_2$ for 30–45 min at 37 °C before recording. The aCSF contained (in mM) 1.25 KCl, 125 NaCl, 1.25 KH$_2$PO$_4$, 25 NaHCO$_3$, 25 D-glucose, 1 MgCl$_2$ and 2 CaCl$_2$ supplemented with 0.4 L-ascorbic acid and 2 Na-pyruvate. All the chemicals were purchased from Sigma.

### 2.4. Whole-cell patch-clamp recordings

#### 2.4.1. Whole-cell patch-clamp recordings

The recordings were performed using oxygenated aCSF solutions at room temperature (~25 °C). Neurons were observed by an upright microscope using a × 40 water-immersion objective lens (FN26.5, Olympus, Japan). The neurons in the VLPO were selected for electrophysiological evaluation. Patch pipettes (5–7 MΩ) were retrieved from borosilicate glass capillaries using a horizontal pipette puller (P-97, Sutter Instruments, USA). The recordings were obtained using a Multiclamp 700B amplifier and analyzed using Clampfit 10.6 software (Molecular Devices). The aCSF was flushed at a specific rate (2 mL/min). Neurons at −60 mV were used to record action potentials using the current-clamp mode. For action potential recording (except Fig. 7A), a potassium-based internal solution containing (in mM) 135 potassium gluconate, 0.1 EGTA, 10 HEPES, 10 KCl, 0.5 Na-GTP and 5 Mg-ATP was used in patch pipettes. The pH was adjusted to 7.2 with KOH. The osmolarity was set to $310 \pm 5$ mOsm kg−1. Neurons at −60 mV were used to record spontaneous

inhibitory postsynaptic currents (sIPSCs) and miniature inhibitory postsynaptic currents (mIPSCs) using the voltage-clamp mode. For sIPSCs and mIPSCs recordings, a high-chloride cesium-based internal solution containing (in mM) 140 CsCl, 10 HEPES, 5 Mg-ATP, 0.5 Na-GTP, and 1 EGTA was used in patch pipettes. The pH was adjusted to 7.2 with CsOH. The osmolarity was set to $310 \pm 5$ mOsm kg$^{-1}$ with CsCl. The bath solution plus 20 μM CNQX, 20 μM D-AP5 was used to record sIPSCs. The bath solution plus 20 μM CNQX, 20 μM D-AP5, and 400 nM TTX was used to record mIPSCs. Baseline recordings were obtained at least 5 min before drug use. Data were sampled at 20 kHz and filtered at 10 kHz.

### 2.4.2. Identification for LTS cells in the voltage-clamp mode

The locus coeruleus (LC) have been verified to project NAergic terminals to the VLPO, which results that NAergic terminals release NA to the VLPO neurons. Two-thirds of VLPO neurons with a low-threshold spike (LTS) are multipolar triangular and inhibited by NA;
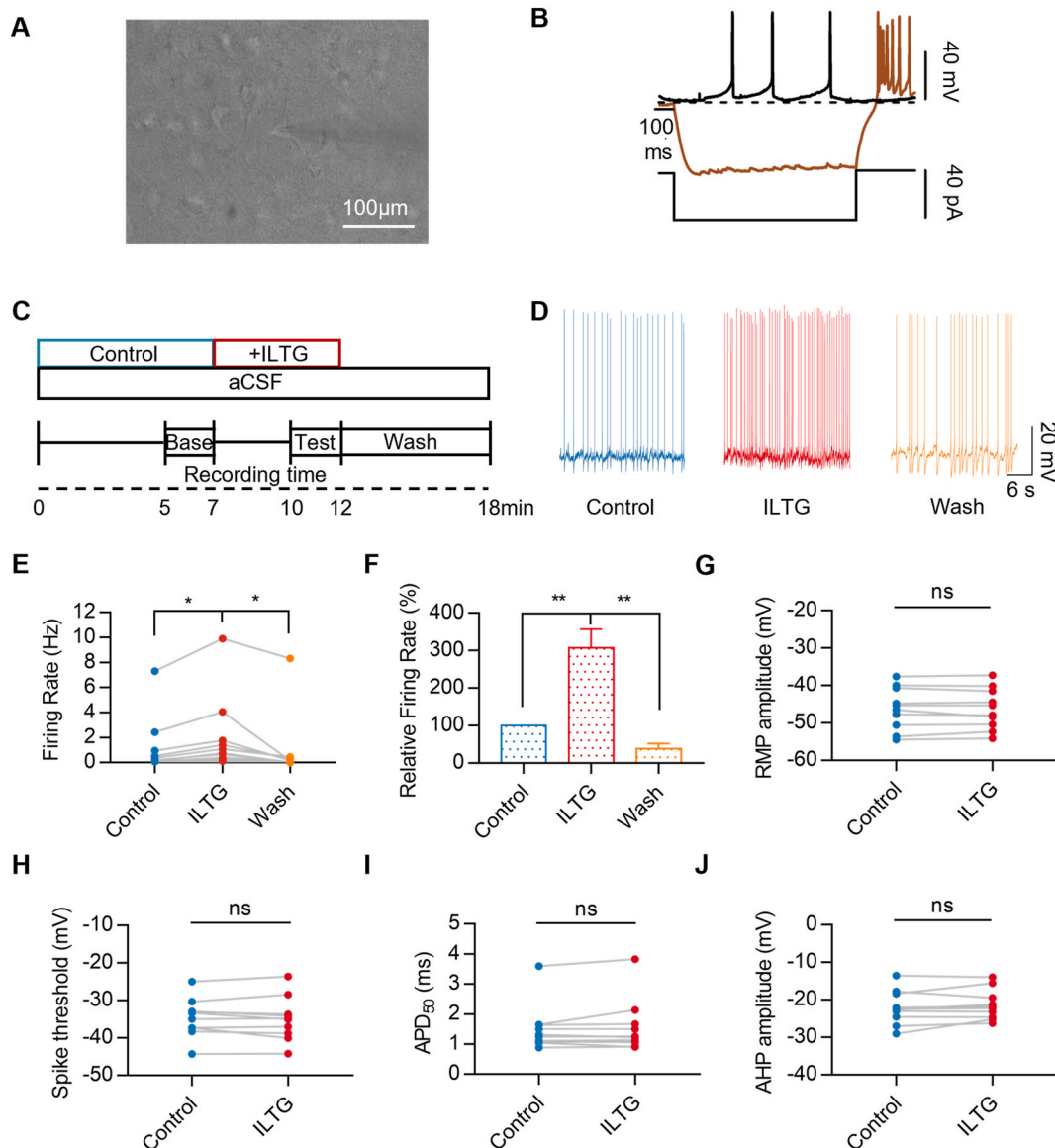


**Fig. 1.** ILTG excites LTS cells of VLPO. (A) A multipolar triangular cell during the whole-cell recording. Scale bar: 100 μm. (B) LTS cells are characterized by a low-threshold spike when depolarized from a hyperpolarized level (−60 pA current stimulus). (C) Experimental procedure of electrophysiological experiments. We recorded action potentials for 18 min on a LTS cell. 5–7 min of control and 10–12 min of ILTG (10 μM) were selected for statistical analysis. (D) Representative traces of action potential of a LTS cell of the VLPO after ILTG (10 μM) perfusion. (E) Statistical results for firing rate after ILTG (10 μM) administration in VLPO LTS cells (one-way ANOVA; n = 11 cells; *P < 0.05). (F) Statistical results for relative firing rate after ILTG (10 μM) administration in VLPO LTS cells (one-way ANOVA; n = 11 cells; **P < 0.01). Error bars indicate the SEM. (G–J) The effect of ILTG (10 μM) on the intrinsic properties of the action potentials of VLPO LTS cells, including RMP amplitude, spike threshold, AHP, and APD$_{50}$ (Paired *t*-test; n = 10 cells).

the remaining cells lack an LTS, which are fusiform and bipolar and excited by NA [18]. Optogenetic activation of NAergic terminals in the locus coeruleus and the perfusion of NA are equivalent. Previous reports [19] have suggested that the optogenetic activation of NAergic terminals in the LC inhibited LTS cells in the VLPO and increased the frequency and amplitude of sIPSCs in VLPO LTS cells, and the perfusion of NA (100 μM) also increased the frequency and amplitude of sIPSCs in VLPO LTS cells. Thus, this study provides new ideas for identifying the characteristics of VLPO LTS cells in the voltage-clamp mode by applying NA (100 μM), resulting in an increase in the frequency of sIPSCs.

### 2.4.3. Experimental procedure of LTS cells in the voltage-clamp mode

sIPSCs and mIPSCs were recorded in sections 3.5 and 3.6 respectively in LTS cells. First, the bath solution plus 20 μM CNQX, 20 μM D-AP5 was used to record sIPSCs for identification of LTS cells for 18 min (Fig. 5A). Then, the bath solution plus 20 μM CNQX, 20 μM D-
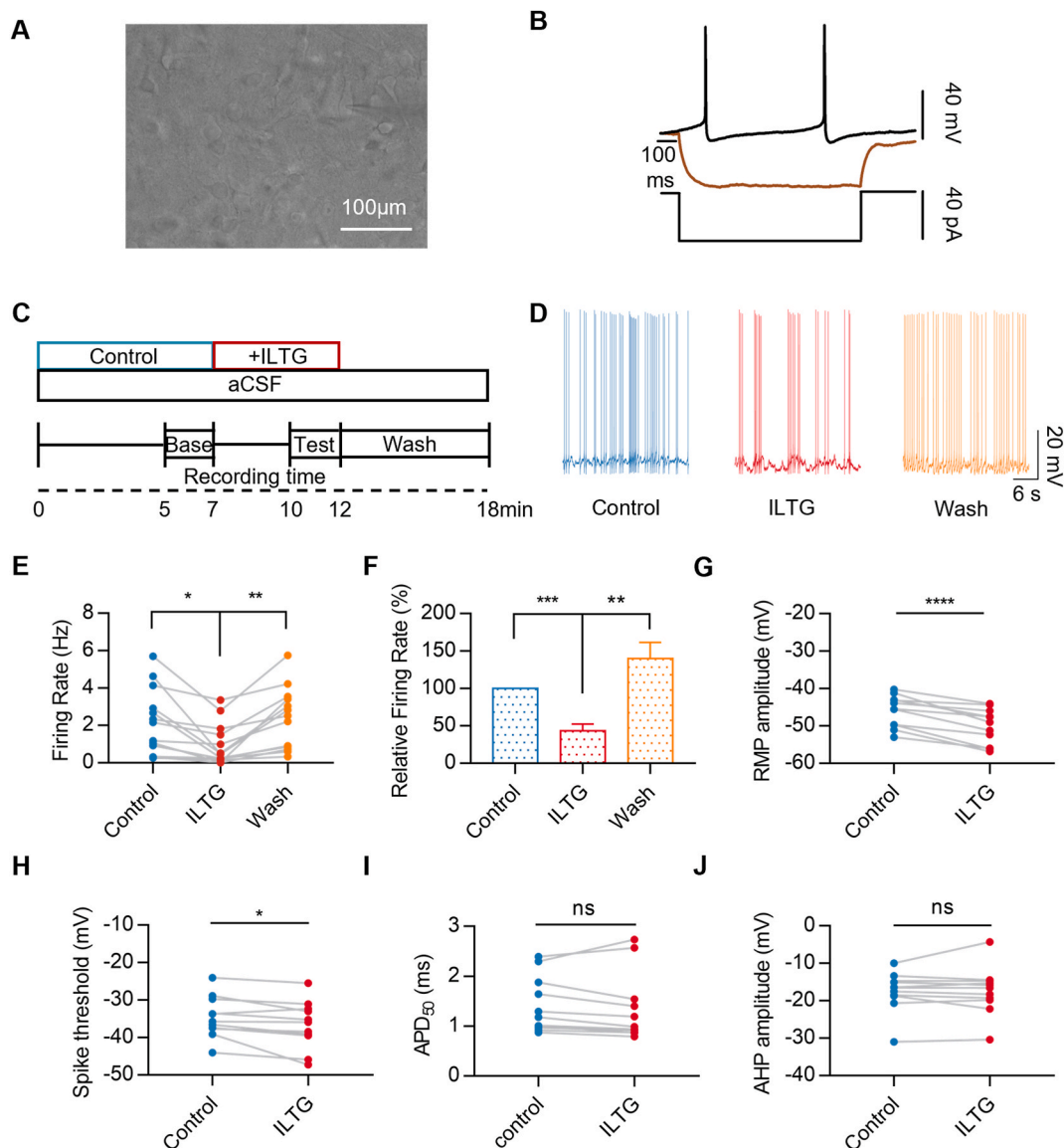


**Fig. 2.** ILTG decreases non-LTS cells of VLPO excitability. (A) A bipolar cell during the whole-cell recording. Scale bar: 100 μm. (B) Non-LTS cells lack an LTS when depolarized from a hyperpolarized level (−60 pA current stimulus). (C) Experimental procedure of electrophysiological experiments. We recorded action potentials for 18 min on a non-LTS cell. 5–7 min of control and 10–12 min of ILTG (10 μM) were selected for statistical analysis. (D) Typical action potential traces of a non-LTS cell of the VLPO after ILTG (10 μM) perfusion. (E) Statistical results for firing rate after ILTG (10 μM) administration in VLPO non-LTS cells (one-way ANOVA; n = 13 cells; *P < 0.05, **P < 0.01). (F) Statistical results for relative firing rate after ILTG (10 μM) administration in VLPO non-LTS cells (one-way ANOVA; n = 13 cells; **P < 0.01, ***P < 0.001). Error bars indicate the SEM. (G–J) The effect of ILTG (10 μM) on the intrinsic properties of the action potentials of VLPO non-LTS cells, including RMP amplitude (****P < 0.0001), spike threshold (*P < 0.05), AHP, and APD$_{50}$. Paired t-test; n = 11 cells.

AP5, and 400 nM TTX was used to record mIPSCs for exploring the effect of ILTG for 18 min (Fig. 6A).

#### 2.4.4. Experimental procedure of non-LTS cells in the voltage-clamp mode

When we used a hyperpolarized current stimulus to record the firing characteristics of non-LTS cells in the VLPO only in Fig. 7A, a high-chloride cesium-based internal solution was filled in patch pipettes to further record mIPSCs on the same cell (The action potential appeared abnormal and was used only to identify non-LTS cells). We first recorded action potential in aCSF to identify non-LTS cells only in Fig. 7A, and then the aCSF plus 20 μM CNQX, 20 μM D-AP5, and 400 nM TTX was used to record mIPSCs for 18 min (Fig. 7A).

### 2.5. Data analysis

Spike threshold was measured at the point during the upstroke (depolarizing phase) of the action potential. Action potential durations (APD50) were measured at 50 % repolarization. Afterhyperpolarization (AHP) amplitude was measured in each cell as the difference between spike threshold for action potential generation and the most negative membrane potential.

### 2.6. Statistical analysis

P values were calculated using paired t tests. ANOVA followed by Bonferroni correction was used to calculate P values under multiple conditions. All data are presented as the mean ± standard error of the mean (SEM). $P < 0.05$ was considered to be statistically significant. All data were analyzed using GraphPad Prism 7.0. The data obtained from whole-cell recordings were analyzed using Clampfit software v.10.6 and Igor Pro 6.10 A.
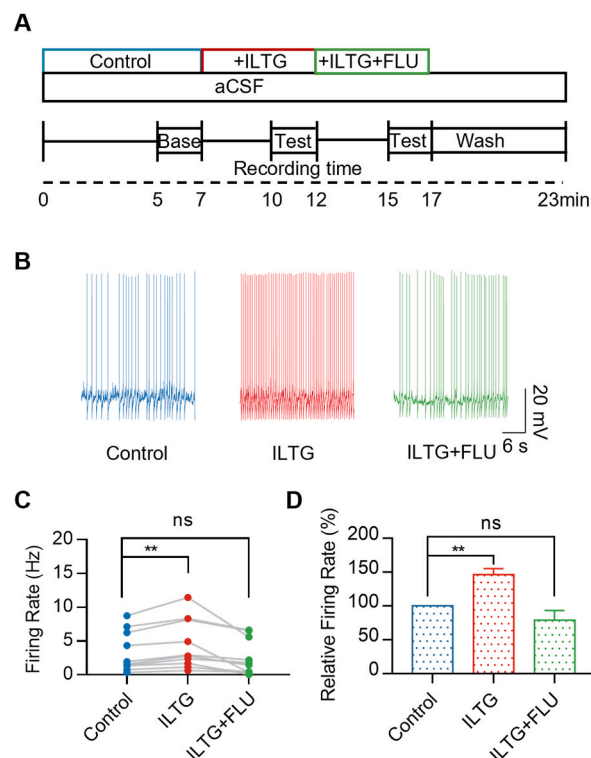


**Fig. 3.** GABA$_A$ receptors mediate ILTG effects on action potential of VLPO LTS cells. (A) Experimental procedure of electrophysiological experiments. We recorded action potentials for 23 min on a LTS cell. 5–7 min of control, 10–12 min of ILTG (10 μM), and 15–17 min of flumazenil (5 μM) were selected for statistical analysis. (B) Typical action potential traces of a LTS cell of the VLPO after ILTG (10 μM), and flumazenil (5 μM) application. (C) Statistical results for firing rate after ILTG (10 μM) and flumazenil (5 μM) application in VLPO LTS cells (one-way ANOVA; n = 10 cells; **P < 0.01). (D) Statistical results for relative firing rate after ILTG (10 μM) and flumazenil (5 μM) application in VLPO LTS cells (one-way ANOVA; n = 10 cells; **P < 0.01). Error bars indicate the SEM.

## 3. Results

### 3.1. ILTG excites LTS cells of VLPO

Previous studies [18,19] have demonstrated that cells in the VLPO can be divided into LTS and non-LTS cells. In whole-cell recordings, the firing characteristics of the LTS and non-LTS cells in the VLPO were different. In this study, we used a hyperpolarized current stimulus to record the firing characteristics of LTS and non-LTS cells in the VLPO. LTS cells were characterized by a potent low-threshold spike with a multipolar triangular morphology, and non-LTS cells lacked an LTS and had a bipolar morphology (Fig. 1A, B, 2A, and 2B).

We evaluated the role of ILTG in VLPO LTS cell firing using brain slice electrophysiological techniques (Fig. 1C). Whole-cell recordings indicated a significant increase in the action potential firing rate of VLPO LTS cells after ILTG (10 µM) perfusion (Fig. 1D). Statistical analysis showed that there was a significant difference in the firing rate before and after ILTG (10 µM) administration (control: $1.103 \pm 0.655$ Hz and ILTG: $1.857 \pm 0.872$ Hz, $P = 0.024$; n = 11 cells; Fig. 1E), which was corresponding to $307.2 \pm 50.4$ % of the control level ($P = 0.006$; n = 11 cells; Fig. 1F). In addition, to observe the effect of ILTG (10 µM) on the intrinsic properties of the action potentials of VLPO LTS cells, we further analyzed RMP amplitude, spike threshold, $APD_{50}$, and AHP amplitude. No difference was detected regarding RMP amplitude, spike threshold, $APD_{50}$, or AHP amplitude after ILTG (10 µM) perfusion (n = 10 cells; Fig. 1G–J). Thus, these data suggest that ILTG excites the LTS cells of the VLPO.

### 3.2. ILTG decreases the excitability of non-LTS cells in the VLPO

We explored the role of ILTG in non-LTS cells in the VLPO firing using brain slice electrophysiological techniques, as depicted in Fig. 2C. Whole-cell recordings indicated a significant decrease in the action potential firing rate of VLPO non-LTS cells after ILTG (10 µM) perfusion (Fig. 2D). Compared to the control group, there was a significant decrease in the firing rate after ILTG (10 µM) administration (control: $2.203 \pm 0.491$ Hz and ILTG: $0.951 \pm 0.306$ Hz, $P = 0.014$; n = 13 cells; Fig. 2E), corresponding to $43.3 \pm 9.2$ % of the control level ($P = 0.001$; n = 13 cells; Fig. 2F). Besides, to observe the effect of ILTG (10 µM) on the intrinsic properties of the action potentials of VLPO non-LTS cells, we further analyzed RMP amplitude, spike threshold, $APD_{50}$, and AHP amplitude. RMP
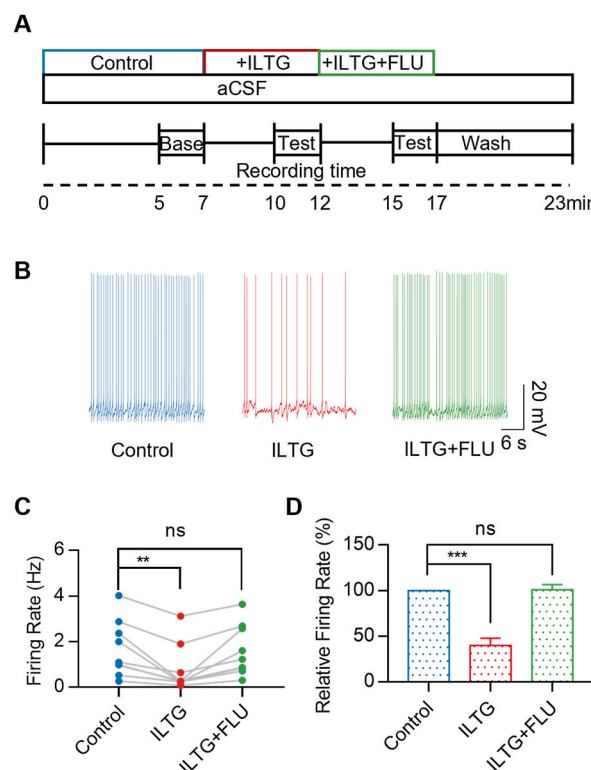


**Fig. 4.** GABA$_A$ receptors mediate ILTG effects on excitability of VLPO non-LTS cells. (A) Experimental procedure of electrophysiological experiments. We recorded action potentials for 23 min on a non-LTS cell. 5–7 min of control, 10–12 min of ILTG (10 µM), and 15–17 min of flumazenil (5 µM) were selected for statistical analysis. (B) Typical action potential traces of a non-LTS cell of the VLPO after ILTG (10 µM), and flumazenil (5 µM) application. (C) Statistical results for firing rate after ILTG (10 µM) and flumazenil (5 µM) application in VLPO non-LTS cells (one-way ANOVA; n = 9 cells; **P < 0.01). (D) Statistical results for relative firing rate after ILTG (10 µM) and flumazenil (5 µM) application in VLPO non-LTS cells (one-way ANOVA; n = 9 cells; ***P < 0.001). Error bars indicate the SEM.

amplitude was more hyperpolarized (control: −46.000 ± 1.281 mV and ILTG: −50.070 ± 1.430 mV, P < 0.0001; n = 11 cells; Fig. 2G) and spike threshold was higher (control: −34.570 ± 1.661 mV and ILTG: −36.640 ± 1.920 mV, P = 0.018; n = 11 cells; Fig. 2H) after ILTG (10 μM) application in VLPO non-LTS cells. No difference was detected in APD$_{50}$, or AHP amplitude (n = 11 cells; Fig. 2I and J) after ILTG application. These data suggest that ILTG decreases VLPO excitability in non-LTS cells.

### 3.3. GABA$_A$ receptors mediate ILTG effects on action potential of VLPO LTS cells

We further investigated the receptor through which ILTG excites the LTS cells of the VLPO, as shown in Fig. 3A. In whole-cell recordings, the increase in neuronal firing caused by ILTG (10 μM) was reversed after flumazenil administration, a GABA$_A$ receptors antagonist (Fig. 3B). As previously described (Fig. 1E), the statistical results demonstrated that the action potential firing rate of VLPO LTS cells showed a significant difference between the control and ILTG (10 μM) (control: 3.391 ± 0.950 Hz and ILTG: 4.463 ± 1.153 Hz, P = 0.005; n = 10 cells; Fig. 3C). Moreover, compared to the control group, there was no difference in the firing rate of VLPO LTS cells after ILTG (10 μM) and flumazenil (5 μM) administration (control: 3.391 ± 0.950 Hz and ILTG + flumazenil: 2.554 ± 0.842 Hz, P = 0.365; n = 10 cells; Fig. 3C), corresponding to 79.0 ± 14.5 % of the control level (P = 0.539; n = 10 cells; Fig. 3D). Our results indicate that GABA$_A$ receptors might mediate the effects of ILTG on the action potential firing of VLPO LTS cells.

### 3.4. GABA$_A$ receptors mediate ILTG effects on the excitability of VLPO non-LTS cells

In addition, we evaluated the receptors through which ILTG decreases the excitability of VLPO non-LTS cells, as shown in Fig. 4A. In whole-cell recordings, the decrease in neuronal firing caused by ILTG (10 μM) was reversed after flumazenil (5 μM) administration (Fig. 4B). As previously described (Fig. 2E), The statistical analysis showed that the action potential firing rate of VLPO non-LTS cells after ILTG (10 μM) application was significantly lower than that from the control group (control: 1.680 ± 0.411 Hz and ILTG: 0.782 ± 0.346 Hz, P = 0.010; n = 9 cells; Fig. 4C). Moreover, compared to the control group, there was no difference in the firing rate of VLPO
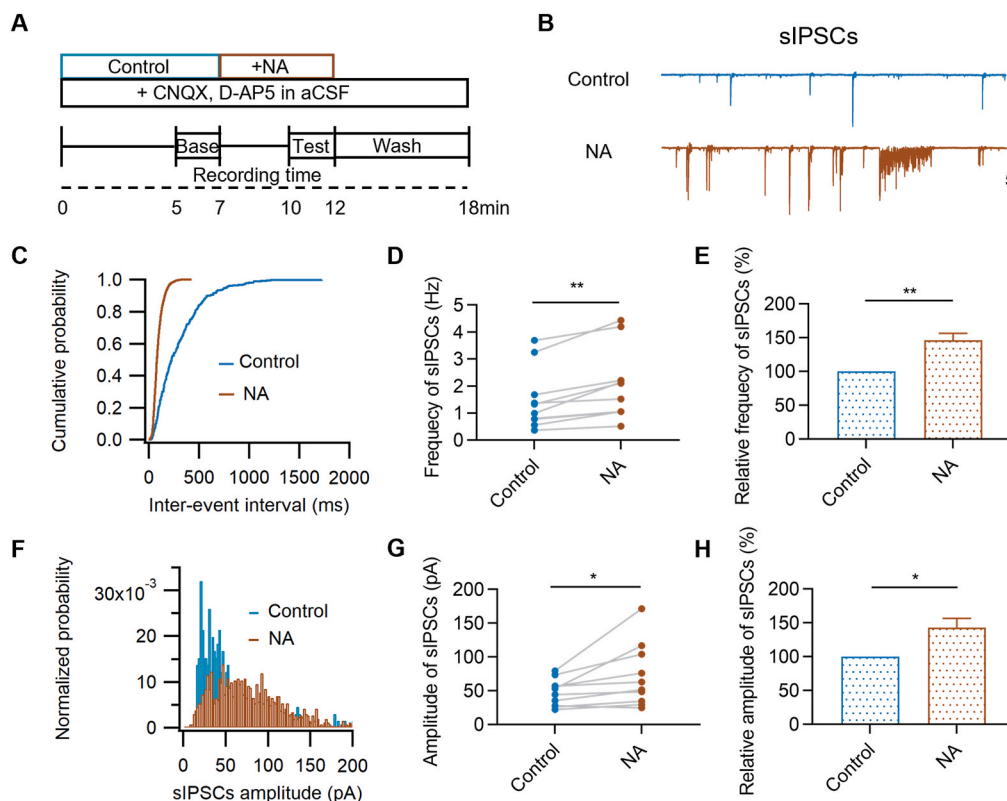


**Fig. 5.** NA increases the frequency and amplitude of sIPSCs in VLPO LTS cells. (A) Experimental procedure of electrophysiological experiments. We recorded sIPSCs for 18 min on a LTS cell. 5–7 min of control and 10–12 min of NA (100 μM) were selected for statistical analysis. (B) Representative sIPSCs traces of a LTS cell of the VLPO after NA (100 μM) perfusion. (C) Cumulative probability of inter-event interval from a LTS cell. (D) Statistical results for the frequency of sIPSCs after NA (100 μM) administration in VLPO LTS cells (paired *t*-test; n = 10 cells; **P < 0.01). (E) Statistical results for the relative frequency of sIPSCs after NA (100 μM) administration in VLPO LTS cells (paired *t*-test; n = 10 cells; **P < 0.01). Error bars indicate the SEM. (F) Normalized probability of amplitude of sIPSCs from a LTS cell. (G) Statistical results for the amplitude of sIPSCs after NA (100 μM) administration in VLPO LTS cells (paired *t*-test; n = 10 cells; *P < 0.05). (H) Statistical results for the relative amplitude of sIPSCs after NA (100 μM) administration in VLPO LTS cells (paired *t*-test; n = 10 cells; *P < 0.05). Error bars indicate the SEM.
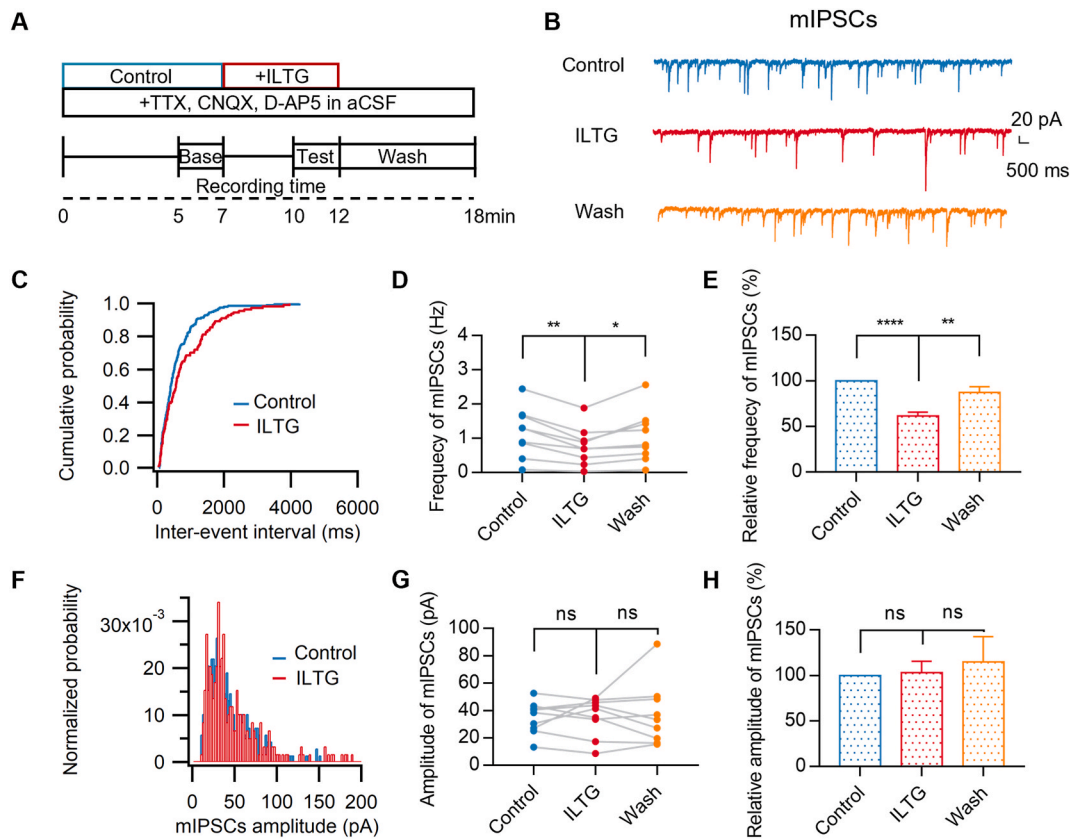
**Fig. 6.** ILTG reduced the frequency of mIPSCs of VLPO LTS cells. (A) Experimental procedure of electrophysiological experiments. We recorded mIPSCs for 18 min on a LTS cell. 5–7 min of control and 10–12 min of ILTG (10 μM) were selected for statistical analysis. (B) Representative mIPSCs traces of a LTS cell of the VLPO after ILTG (10 μM) application. (C) Cumulative probability of inter-event interval from a LTS cell. (D) Statistical results for the frequency of mIPSCs after ILTG (10 μM) administration in VLPO LTS cells (one-way ANOVA; n = 9 cells; *P < 0.05, **P < 0.01). (E) Statistical results for the relative frequency of mIPSCs after ILTG (10 μM) administration in VLPO LTS cells (one-way ANOVA; n = 9 cells; **P < 0.01, ****P < 0.0001). Error bars indicate the SEM. (F) Normalized probability of the amplitude of mIPSCs from a LTS cell. (G) Statistical results for the amplitude of mIPSCs after ILTG (10 μM) administration in VLPO LTS cells (one-way ANOVA; n = 9 cells). (H) Statistical results for relative amplitude of mIPSCs after ILTG (10 μM) administration in VLPO LTS cells (one-way ANOVA; n = 9 cells). Error bars indicate the SEM.

non-LTS cells after ILTG (10 μM) and flumazenil (5 μM) administration (control: 1.680 ± 0.411 Hz and ILTG + flumazenil: 1.610 ± 0.372 Hz, P > 0.999; n = 9 cells; Fig. 4C), corresponding to 101.0 ± 5.7 % of the control level (P > 0.999; n = 9 cells; Fig. 4D). Our results indicate that the effects of ILTG on the excitability of VLPO non-LTS cells might be mediated by GABA$_A$ receptors.

### 3.5. Noradrenaline (NA) increases the frequency and amplitude of sIPSCs of LTS cells in the VLPO

We applied NA in voltage-clamp mode to identify the type of VLPO cells, as depicted in Fig. 5A. Fig. 5B showed the effect of NA (100 μM) on VLPO LTS cells. In the cumulative probability plot, NA (100 μM) shifts the distribution of the inter-event interval to the left (Fig. 5C). The statistical results showed that the frequency of sIPSCs after NA (100 μM) administration was significantly increased than that from the control group (control: 1.482 ± 0.355 Hz and NA: 2.028 ± 0.421 Hz, P = 0.002; n = 10 cells; Fig. 5D), accompanied by 146.2 ± 10.5 % of the control level (P = 0.002; n = 10 cells; Fig. 5E). At the same time, in the normalized probability plot, the amplitude distribution of sIPSCs between the control and NA (100 μM) was different (Fig. 5F). There was a statistically significant increase in the amplitude of sIPSCs after NA (100 μM) administration compared to the control group (control: 47.550 ± 6.284 pA and NA: 71.950 ± 14.690 pA, P = 0.031; n = 10 cells; Fig. 5G), which was corresponding to 142.9 ± 13.5 % of the control level (P = 0.011; n = 10 cells; Fig. 5H). These results provide VLPO LTS cells identification for section 3.6.

### 3.6. ILTG reduced the frequency of mIPSCs of VLPO LTS cells

We first identify VLPO LTS cells in Fig. 5. Then, to check whether the receptor of ILTG acting on VLPO LTS cells is located pre-synaptic or postsynaptic, we perfused TTX (0.4 μM) in the aCSF to eliminate spontaneous action potentials during voltage-clamp recording of postsynaptic currents, and CNQX (20 μM) and D-AP5 (20 μM) to block glutamate receptors, as shown in Fig. 6A. The
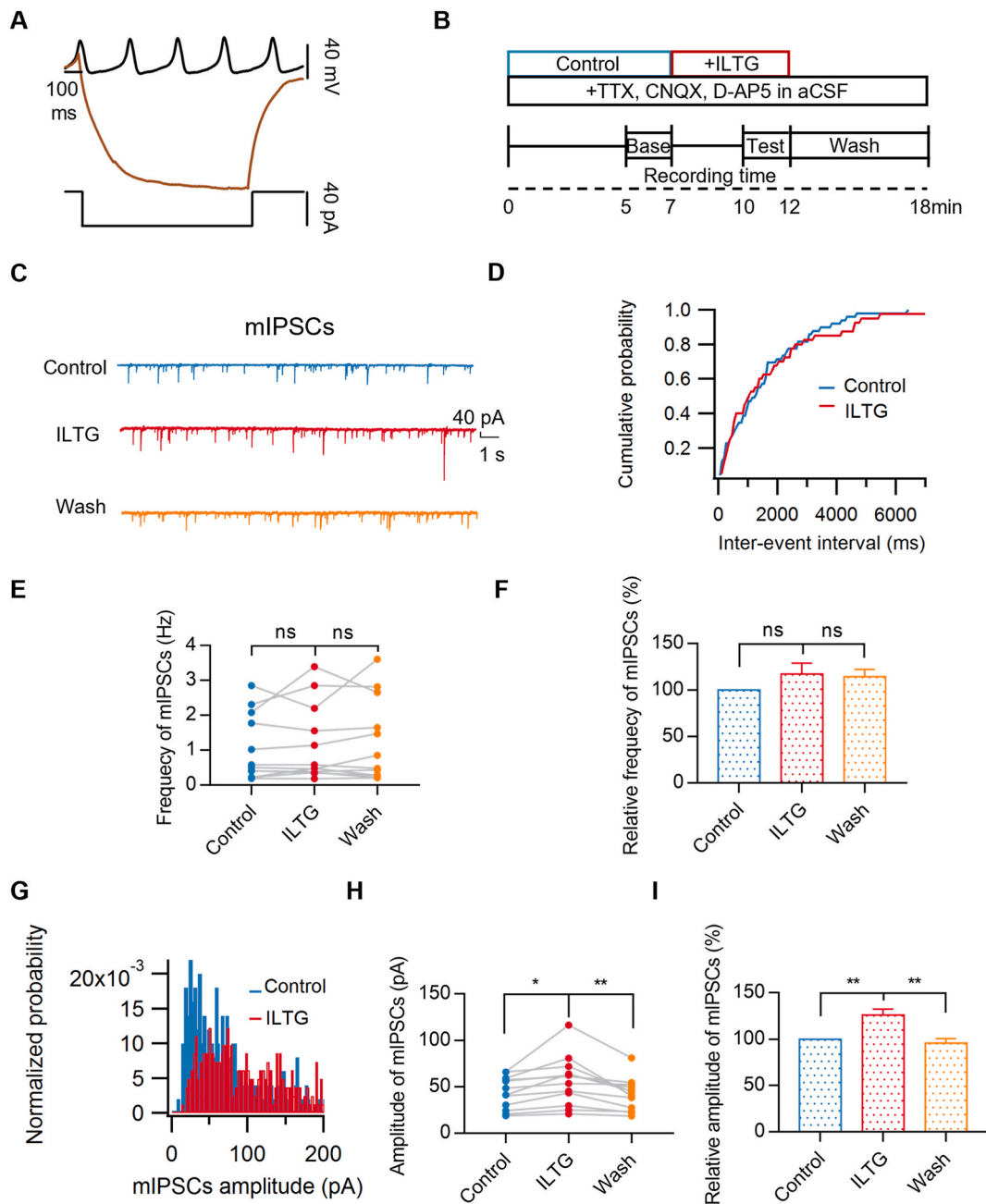
**Fig. 7.** ILTG potentiates the amplitude of mIPSCs of VLPO non-LTS cells. (A) Non-LTS cells lack an LTS when depolarized from a hyperpolarized level (−60 pA current stimulus). (B) Experimental procedure of electrophysiological experiments. We recorded mIPSCs for 18 min on a non-LTS cell. 5–7 min of control and 10–12 min of ILTG (10 μM) were selected for statistical analysis. (C) Representative mIPSCs traces of a non-LTS cell of the VLPO after ILTG (10 μM) application. (D) Cumulative probability of inter-event interval from a non-LTS cell. (E) Statistical results for the frequency of mIPSCs after ILTG (10 μM) administration in VLPO non-LTS cells (one-way ANOVA; n = 12 cells). (F) Statistical results for the relative frequency of mIPSCs after ILTG (10 μM) administration in VLPO non-LTS cells (one-way ANOVA; n = 12 cells). Error bars indicate the SEM. (G) Normalized probability of amplitude of mIPSCs from a non-LTS cell. (H) Statistical results for the amplitude of mIPSCs after ILTG (10 μM) administration in VLPO non-LTS cells (one-way ANOVA; n = 12 cells; *P < 0.05, **P < 0.01). (I) Statistical results for the relative amplitude of mIPSCs after ILTG (10 μM) administration in VLPO non-LTS cells (one-way ANOVA; n = 12 cells; **P < 0.01). Error bars indicate the SEM.

effect of ILTG (10 μM) on VLPO LTS cells was shown in Fig. 6B. In the cumulative probability plot, ILTG (10 μM) caused the distribution of the inter-event interval to shift to the right (Fig. 6C). The statistical analysis showed that the frequency of mIPSCs after ILTG (10 μM) application was significantly lower than that from the control group (control: 1.177 ± 0.239 Hz and ILTG: 0.772 ± 0.182 Hz, P = 0.002; n = 9 cells; Fig. 6D), corresponding to 61.3 ± 4.4 % of the control level (P < 0.0001; n = 9 cells; Fig. 6E). Meanwhile, in the

normalized probability plot, no difference in the amplitude distribution of mIPSCs between the control and ILTG (10 μM) was observed (Fig. 6F). The statistical results showed that the amplitude of mIPSCs after ILTG (10 μM) perfusion was the same as that from the control group (control: 34.690 ± 3.943 pA and ILTG: 35.790 ± 4.726 pA, P > 0.9999; n = 9 cells; Fig. 6G), accompanied by 103.2 ± 12.4 % of the control level (P > 0.9999; n = 9 cells; Fig. 6H). Therefore, our results reveal that ILTG suppresses presynaptic GABA release on VLPO LTS cells.

### 3.7. ILTG potentiates the amplitude of mIPSCs of VLPO non-LTS cells

We used a hyperpolarized current stimulus to record the firing characteristics of non-LTS cells in the VLPO in Fig. 7A. At the same time, a high-chloride cesium-based internal solution was filled in patch pipettes to further record mIPSCs on the same cell. Non-LTS cells lacked an LTS. To check whether the receptor of ILTG acting on VLPO non-LTS cells is located presynaptic or postsynaptic, we perfused TTX (0.4 μM) in the aCSF to eliminate spontaneous action potentials during voltage-clamp recording of postsynaptic currents, and CNQX (20 μM) and D-AP5 (20 μM) to block glutamate receptors, as shown in Fig. 7B. The effect of ILTG (10 μM) on VLPO non-LTS cells was shown in Fig. 7C. In the cumulative probability plot, no difference in the distribution of the inter-event interval between the control and ILTG (10 μM) was observed (Fig. 7D). The statistical results showed that the frequency of mIPSCs after ILTG (10 μM) perfusion was the same as that from the control group (control: 1.047 ± 0.273 Hz and ILTG: 1.161 ± 0.317 Hz, P > 0.9999; n = 12 cells; Fig. 7E), corresponding to 117.0 ± 12.0 % of the control level (P = 0.550; n = 12 cells; Fig. 7F). Meanwhile, in the normalized probability plot, the amplitude distribution of mIPSCs between the control and ILTG (10 μM) was different (Fig. 7G). The statistical analysis showed that the amplitude of mIPSCs after ILTG (10 μM) application was significantly higher than that from the control group (control: 44.070 ± 5.041 pA and ILTG: 56.170 ± 7.702 pA, P = 0.033; n = 12 cells; Fig. 7H), accompanied by 126.2 ± 6.3 % of the control level (P = 0.005; n = 12 cells; Fig. 7I). Therefore, our results reveal that ILTG enhances postsynaptic GABA$_A$ receptor function on VLPO non-LTS cells.

## 4. Discussion

This study aimed to explore the influence of ILTG on LTS and non-LTS cells in the VLPO using whole-cell patch clamp recording. Our results showed that the effect of ILTG on LTS and non-LTS cells in the VLPO was different. ILTG suppresses presynaptic GABA release on VLPO LTS cells, thereby increasing their excitability. ILTG enhances postsynaptic GABA$_A$ receptor function on VLPO non-LTS cells, thereby decreasing their excitability.

Cho et al. have revealed that ILTG shows hypnotic function via GABA$_A$ receptors, which may inhibit the dorsal raphe (DR) neurons, one of the arousal centers [12]. VLPO is a sleep-promoting center and appears to contain most of the GABA-released cells [14–17,21, 23]. Moreover, GABAergic synaptic transmission in the VLPO regulates the sleep-wake state [21,23]. However, the effects of ILTG on both cell types in the VLPO remain still unknown.

The VLPO is a sleep-promoting region in which LTS cells play a role in sleep, accounting for approximately two-thirds of the VLPO [18,19,29]. Previous studies indicated that most LTS cells co-release GABA and galanin [21]. Meanwhile, VLPO as a sleep-promoting function is mainly attributed to galaninergic neurons [21,30]. Our results showed that ILTG excited sleep-promoting LTS cells, approximately 307.2 ± 50.4 % of the control level, which may coincide with its hypnotic effect. Furthermore, compared to the control group, there was no difference in the firing rate of VLPO LTS cells after ILTG and flumazenil administration, which indicated that GABA$_A$ receptors mediate the effects of ILTG on the action potential of VLPO LTS cells. The statistical analysis showed that the frequency of mIPSCs after ILTG application was significantly lower than that from the control group. Studies have shown that acutely activated wake-promoting GABAergic neurons in the lateral hypothalamus and the galaninergic neurons in the VLPO are inhibited, resulting in arousal [23–25]. In addition, studies have shown that orexin, histamine, and other wake-up signals may inhibit galaninergic neurons in the VLPO via internal GABAergic circuits [19,22,26–28]. There may be presynaptic inhibition. The sleep-promoting effect of ILTG on LTS cells might be through presynaptic inhibitions, thereby increasing their excitability. These results indicate that ILTG suppresses presynaptic GABA release on VLPO LTS cells, thereby increasing their excitability.

The remaining cells in the VLPO are non-LTS cells, which are wake-promoting [18,19]. Our results indicated that ILTG decreased the excitability of non-LTS cells, approximately 43.3 ± 9.2 % of the control level, which may explain the hypnotic effect of ILTG. Moreover, compared to the control group, there was no difference in the firing rate of VLPO non-LTS cells after ILTG and flumazenil administration. This study also showed that ILTG reduced the RMP amplitude and enhanced the spike threshold in VLPO non-LTS cells. The statistical analysis showed that the amplitude of mIPSCs after ILTG application was significantly higher than that from the control group. Studies have shown that most VLPO cells contain GABA [21,23]. These results indicate that ILTG enhances postsynaptic GABA$_A$ receptor function on VLPO non-LTS cells, thereby decreasing their excitability.

ILTG has many pharmacological effects, among which the function of hypnosis is equally important. Here, we examined the influence of ILTG on LTS and non-LTS cells in the VLPO. Studies have shown that most LTS cells are sleep-promoting and most non-LTS cells are arousal-promoting [19]. Consistently, ILTG excites LTS cells of VLPO, while decreases VLPO excitability in non-LTS cells. Functionally, this confirmed the hypnotic function of ILTG. This may provide more clarity on the hypnotic mechanism and identify a potential target for the hypnotic effect of ILTG, thereby contributing to the development of ILTG as a hypnotic drug.

In summary, ILTG suppresses presynaptic GABA release on VLPO LTS cells, thereby increasing their excitability. ILTG enhances postsynaptic GABA$_A$ receptor function on VLPO non-LTS cells, thereby decreasing their excitability. These results suggest that ILTG may produce hypnotic effects by modulating the GABAergic synaptic transmission properties of these two cell types.

## Data availability statement

Data will be made available on request.

## Additional information

No additional information is available for this paper.

## CRediT authorship contribution statement

**Sumei Fan:** Performed the experiments, Analyzed and interpreted the data; Wrote the paper. **Qiaoling Jin:** Analyzed and interpreted the data.. **Pingping Zhang:** Analyzed and interpreted the data.. **Dejiao Xu:** Analyzed and interpreted the data.. **Juan Cheng:** Conceived and designed the experiments; Contributed reagents, materials, analysis tools or data, Wrote the paper. **Liecheng Wang:** Conceived and designed the experiments; Contributed reagents, materials, analysis tools or data, Wrote the paper.

## Declaration of competing interest

The authors declare that they have no known competing financial interests or personal relationships that could have appeared to influence the work reported in this paper.

## Acknowledgments

## References

[1] K.L. Wang, Y.C. Yu, S.M. Hsia, Perspectives on the role of isoliquiritigenin in cancer, Cancers 13 (1) (2021) 115, https://doi.org/10.3390/cancers13010115.

[2] C.Y. Lin, Y.C. Lin, C.R. Paul, D.J.Y. Hsieh, C.H. Day, R.J. Chen, C.H. Kuo, T.J. Ho, M.A. Shibu, C.H. Lai, T.C. Shih, W.W. Kuo, C.Y. Huang, Isoliquiritigenin ameliorates advanced glycation end-products toxicity on renal proximal tubular epithelial cells, Environ. Toxicol. 37 (8) (2022) 2096–2102, https://doi.org/10.1002/tox.23553.

[3] Z. Zhang, W.Q. Chen, S.Q. Zhang, J.X. Bai, B. Liu, K.K.L. Yung, J.K.S. Ko, Isoliquiritigenin inhibits pancreatic cancer progression through blockade of p38 MAPK-regulated autophagy, Phytomedicine 106 (2022), 154406, https://doi.org/10.1016/j.phymed.2022.154406.

[4] J. Zeng, W. Liu, B. Liang, L. Shi, S. Yang, J. Meng, J. Chang, X. Hu, R. Zhang, D. Xing, Inhibitory effect of isoliquiritigenin in niemann-pick C1-like 1-mediated cholesterol uptake, Molecules 27 (21) (2022) 7494, https://doi.org/10.3390/molecules27217494.

[5] Z. Song, Y. Zhang, H. Zhang, R.S. Rajendran, R. Wang, C.D. Hsiao, J. Li, Q. Xia, K. Liu, Isoliquiritigenin triggers developmental toxicity and oxidative stress–mediated apoptosis in zebrafish embryos/larvae via Nrf2-HO1/JNK-ERK/mitochondrion pathway, Chemosphere 246 (2020), 125727, https://doi.org/10.1016/j.chemosphere.2019.125727.

[6] Y. Fu, J. Jia, Isoliquiritigenin confers neuroprotection and alleviates amyloid-β42-induced neuroinflammation in microglia by regulating the Nrf2/NF-κB signaling, Front. Neurosci. 15 (2021), 638772, https://doi.org/10.3389/fnins.2021.638772.

[7] X. Zhu, J. Liu, O. Chen, J. Xue, S. Huang, W. Zhu, Y. Wang, Neuroprotective and anti-inflammatory effects of isoliquiritigenin in kainic acid-induced epileptic rats via the TLR4/MYD88 signaling pathway, Inflammopharmacology 27 (2019) 1143–1153, https://doi.org/10.1007/s10787-019-00592-7.

[8] R. Prajapati, S.H. Seong, S.E. Park, P. Paudel, H.A. Jung, J.S. Choi, Isoliquiritigenin, a potent human monoamine oxidase inhibitor, modulates dopamine D1, D3, and vasopressin V1A receptors, Sci. Rep. 11 (1) (2021), 23528, https://doi.org/10.1038/s41598-021-02843-6.

[9] H.J. Park, H.S. Shim, H. Kim, K.S. Kim, H. Lee, D.H. Hahm, I. Shim, Effects of Glycyrrhiza Radix on repeated restraint stress-induced neurochemical and behavioral responses, Korean J. Physiol. Pharmacol. 14 (6) (2010) 371–376, https://doi.org/10.4196/kjpp.2010.14.6.371.

[10] Y. Wang, S.C. Kim, T. Wu, Y. Jiao, H. Jin, B. Hyo Lee, C. Won Lee, Y. Fan, H.Y. Kim, C.H. Yang, Z. Zhao, R. Zhao, Isoliquiritigenin attenuates anxiety-like behavior and locomotor sensitization in rats after repeated exposure to nicotine, Evid. Based. Complement. Alternat. Med. (2020), https://doi.org/10.1155/2020/9692321.

[11] O.O. Adeyemi, A.J. Akindele, O.K. Yemitan, F.R. Aigbe, F.I. Fagbo, Anticonvulsant, anxiolytic and sedative activities of the aqueous root extract of Securidaca longepedunculata Fresen, J. Ethnopharmacol. 130 (2) (2010) 191–195, https://doi.org/10.1016/j.jep.2010.04.028.

[12] S. Cho, S. Kim, Z. Jin, H. Yang, D. Han, N.I. Baek, J. Jo, C. Cho, J. Park, M. Shimizu, Y.H. Jin, Isoliquiritigenin, a chalcone compound, is a positive allosteric modulator of GABAA receptors and shows hypnotic effects, Biochem. Biophys. Res. Commun. 413 (4) (2011) 637–642, https://doi.org/10.1016/j.bbrc.2011.09.026.

[13] J. Woo, S. Cho, C.J. Lee, Isoliquiritigenin, a chalcone compound, enhances spontaneous inhibitory postsynaptic response, Exp. Neurobiol. 23 (2) (2014) 163, https://doi.org/10.5607/en.2014.23.2.163.

[14] Y.C. Saito, T. Maejima, M. Nishitani, E. Hasegawa, Y. Yanagawa, M. Mieda, T. Sakurai, Monoamines inhibit GABAergic neurons in ventrolateral preoptic area that make direct synaptic connections to hypothalamic arousal neurons, J. Neurosci. 38 (28) (2018) 6366–6378, https://doi.org/10.1523/jneurosci.2835-17.2018.

[15] S. Teng, F. Zhen, L. Wang, J.C. Schalchli, J. Simko, X. Chen, H. Jin, C.D. Makinson, Y. Peng, Control of non-REM sleep by ventrolateral medulla glutamatergic neurons projecting to the preoptic area, Nat. Commun. 13 (1) (2022) 4748, https://doi.org/10.1038/s41467-022-32461-3.

[16] F. Lombardi, M. Gómez-Extremera, P. Bernaola-Galván, R. Vetrivelan, C.B. Saper, T.E. Scammell, P.C. Ivanov, Critical dynamics and coupling in bursts of cortical rhythms indicate non-homeostatic mechanism for sleep-stage transitions and dual role of VLPO neurons in both sleep and wake, J. Neurosci. 40 (1) (2020) 171–190, https://doi.org/10.1523/jneurosci.1278-19.2019.

[17] J.H. Kim, I.S. Choi, J.Y. Jeong, I.S. Jang, M.G. Lee, K. Suk, Astrocytes in the ventrolateral preoptic area promote sleep, J. Neurosci. 40 (47) (2020) 8994–9011, https://doi.org/10.1523/jneurosci.1486-20.2020.

[18] T. Gallopin, P. Fort, E. Eggermann, B. Cauli, P.H. Luppi, J. Rossier, E. Audinat, M. Mühlethaler, M. Serafin, Identification of sleep-promoting neurons in vitro, Nature 404 (6781) (2000) 992–995, https://doi.org/10.1038/35010109.

[19] Y. Liang, W. Shi, A. Xiang, D. Hu, L. Wang, L. Zhang, The NAergic locus coeruleus-ventrolateral preoptic area neural circuit mediates rapid arousal from sleep, Curr. Biol. 31 (17) (2021) 3729–3742, https://doi.org/10.1016/j.cub.2021.06.031.

[20] A. Sangare, R. Dubourget, H. Geoffroy, T. Gallopin, A. Rancillac, Serotonin differentially modulates excitatory and inhibitory synaptic inputs to putative sleep-promoting neurons of the ventrolateral preoptic nucleus, Neuropharmacology 109 (2016) 29–40, https://doi.org/10.1016/j.neuropharm.2016.05.015.

[21] D. Kroeger, G. Absi, C. Gagliardi, S.S. Bandaru, J.C. Madara, L.L. Ferrari, E. Arrigoni, H. Münzberg, T.E. Scammell, C.B. Saper, R. Vetrivelan, Galanin neurons in the ventrolateral preoptic area promote sleep and heat loss in mice, Nat. Commun. 9 (1) (2018) 4129, https://doi.org/10.1038/s41467-018-06590-7.

[22] Y.W. Liu, J. Li, J.H. Ye, Histamine regulates activities of neurons in the ventrolateral preoptic nucleus, J. Physiol. 588 (21) (2010) 4103–4116, https://doi.org/10.1113/jphysiol.2010.193904.

[23] E. Arrigoni, P.M. Fuller, The sleep-promoting ventrolateral preoptic nucleus: what have we learned over the past 25 Years? Int. J. Mol. Sci. 23 (6) (2022) 2905, https://doi.org/10.3390/ijms23062905.

[24] A. Venner, C. Anaclet, R.Y. Broadhurst, C.B. Saper, P.M. Fuller, A novel population of wake-promoting GABAergic neurons in the ventral lateral hypothalamus, Curr. Biol. 26 (16) (2016) 2137–2143, https://doi.org/10.1016/j.cub.2016.05.078.

[25] A. Venner, R. De Luca, L.T. Sohn, S.S. Bandaru, A.M. Verstegen, E. Arrigoni, P.M. Fuller, An inhibitory lateral hypothalamic-preoptic circuit mediates rapid arousals from sleep, Curr. Biol. 29 (24) (2019) 4155–4168, https://doi.org/10.1016/j.cub.2019.10.026.

[26] R.H. Williams, M.J. Chee, D. Kroeger, L.L. Ferrari, E. Maratos-Flier, T.E. Scammell, E. Arrigoni, Optogenetic-mediated release of histamine reveals distal and autoregulatory mechanisms for controlling arousal, J. Neurosci. 34 (17) (2014) 6023–6029, https://doi.org/10.1523/jneurosci.4838-13.2014.

[27] R. De Luca, D. Park, S. Bandaru, E. Arrigoni, Orexin mediates feed-forward inhibition of VLPO sleep-active neurons-a mechanism for controlling arousal, J. Sleep Sleep Disord. Res. 40 (suppl_1) (2017), https://doi.org/10.1093/sleepj/zsx050.133. A50-A50.

[28] Z. Zhang, V. Ferretti, İ. Güntan, A. Moro, E.A. Steinberg, Z. Ye, A.Y. Zecharia, X. Yu, A.L. Vyssotski, S.G. Brickley, R. Yustos, Z.E. Pillidge, E.C. Harding, W. Wisden, N.P. Franks, Neuronal ensembles sufficient for recovery sleep and the sedative actions of α2 adrenergic agonists, Nat. Neurosci. 18 (4) (2015) 553–561, https://doi.org/10.1038/nn.3957.

[29] R. Dubourget, A. Sangare, H. Geoffroy, T. Gallopin, A. Rancillac, Multiparametric characterization of neuronal subpopulations in the ventrolateral preoptic nucleus, Brain Struct. Funct. 222 (2017) 1153–1167, https://doi.org/10.1007/s00429-016-1265-2.

[30] I.S. Choi, J.H. Kim, J.Y. Jeong, M.G. Lee, K. Suk, I.S. Jang, Astrocyte-derived adenosine excites sleep-promoting neurons in the ventrolateral preoptic nucleus: astrocyte-neuron interactions in the regulation of sleep, Glia 70 (10) (2022) 1864–1885, https://doi.org/10.1002/glia.24225.